Journal of Cell Science 108, 2311-2320 (1995)
Printed in Great Britain © The Company of Biologists Limited 1995

Cytoskeletal filament assembly and the control of cell spreading and function by extracellular matrix

David J. Mooney[1,2,*], Robert Langer[1,2] and Donald E. Ingber[2,3,†]

[1]Department of Chemical Engineering, Massachusetts Institute of Technology, Cambridge, MA, USA
Departments of [2]Surgery and [3]Pathology, Children's Hospital and Harvard Medical School, Boston, MA, USA

*Present address: Departments of Biologic and Materials Sciences and Chemical Engineering, University of Michigan, Ann Arbor, MI, USA
†Author for correspondence at: The Children's Hospital, Enders 1007, 300 Longwood Avenue, Boston, MA 02115, USA

SUMMARY

This study was undertaken to analyze how cell binding to extracellular matrix produces changes in cell shape. We focused on the initial process of cell spreading that follows cell attachment to matrix and, thus, cell 'shape' changes are defined here in terms of alterations in projected cell areas, as determined by computerized image analysis. Cell spreading kinetics and changes in microtubule and actin microfilament mass were simultaneously quantitated in hepatocytes plated on different extracellular matrix substrata. The initial rate of cell spreading was highly dependent on the matrix coating density and decreased from 740 $\mu m^2/h$ to 50 $\mu m^2/h$ as the coating density was lowered from 1000 to 1 ng/cm^2. At approximately 4 to 6 hours after plating, this initial rapid spreading rate slowed and became independent of the matrix density regardless of whether laminin, fibronectin, type I collagen or type IV collagen was used for cell attachment. Analysis of F-actin mass revealed that cell adhesion to extracellular matrix resulted in a 20-fold increase in polymerized actin within 30 minutes after plating, before any significant change in cell shape was observed. This was followed by a phase of actin microfilament disassembly which correlated with the most rapid phase of cell extension and ended at about 6 hours; F-actin mass remained relatively constant during the slow matrix-independent spreading phase. Microtubule mass increased more slowly in spreading cells, peaking at 4 hours, the time at which the transition between rapid and slow spreading rates was observed. However, inhibition of this early rise in microtubule mass using either nocodazole or cycloheximide did not prevent this transition. Use of cytochalasin D revealed that microfilament integrity was absolutely required for hepatocyte spreading whereas interference with microtubule assembly (using nocodazole or taxol) or protein synthesis (using cycloheximide) only partially suppressed cell extension. In contrast, cell spreading could be completely inhibited by combining sub-optimal doses of cytochalasin D and nocodazole, suggesting that intact microtubules can stabilize cell form when the microfilament lattice is partially compromised. The physiological relevance of the cytoskeleton and cell shape in hepatocyte physiology was highlighted by the finding that a short exposure (6 hour) of cells to nocodazole resulted in production of smaller cells 42 hours later that exhibited enhanced production of a liver-specific product (albumin). These data demonstrate that spreading and flattening of the entire cell body is not driven directly by net polymerization of either microfilaments or microtubules. Instead, extracellular matrix appears to control cell shape and function by producing global changes in a structurally integrated cytoskeletal network.

Key words: cell shape, hepatocyte, microtubule, microfilament, differentiation

INTRODUCTION

Many specialized cells, such as hepatocytes, can be switched between growth and differentiation programs by changing the extracellular matrix (ECM) substratum that is used for cell attachment and, thereby, modulating cell shape or extension (Michalopoulos and Pitot, 1975; Folkman and Moscona, 1978; Bissel et al., 1987; Li et al., 1987; Ben Ze'ev et al., 1988; Watt et al., 1988; Ingber and Folkman, 1989a; Opas, 1989; Mooney et al., 1992; Singhvi et al., 1994). While it is known that changes in cell shape are mediated by alterations in the cytoskeleton, the molecular and biophysical basis for these alterations remain unknown. The observation that alterations in actin microfilament (MF) assembly, severing, and cross-linking occur in local regions of the leading edge of migrating cells has led to the concept that actin polymerization events (Stossel, 1989; Theriot and Mitchison, 1991) or sol-gel transformations of the actin lattice (Kolega et al., 1991) act as a driving force for cell extension during locomotion. However, it is not clear that this mechanism is used to promote the global shape changes (i.e. cell spreading and flattening) that are observed when cells first attach to ECM. For example, cells can change from flat to round within a period of seconds (e.g. when trypsinized) without any change in total cellular F-actin

(Bereiter-Hahn et al., 1990). This type of observation has led us to suggest that large-scale changes in cytoskeletal organization and pattern may result from changes in mechanical stresses associated with altered adhesion rather than from polymerization per se (Ingber, 1993; Ingber et al., 1994). In this type of tension-molding mechanism, cell extension is driven by the inward pull of the cytoskeleton being resisted by both internal cytoskeletal struts and external ECM tethers via utilization of a 'tensegrity' mechanism. Thus, in the present study, we set out to ask whether it is net cytoskeletal filament assembly per se or structural remodeling of the pre-existing cytoskeletal lattice that drives the cell shape changes (i.e. spreading or rounding) which are critical for control of hepatocyte function.

To discriminate between these mechanisms, we quantitated changes in cytoskeletal filament assembly that occur following cell attachment to ECM. Primary rat hepatocytes were plated on dishes coated with different densities of purified ECM molecules (laminin, fibronectin, or types I or IV collagens), and both changes in cell shape (i.e. projected cell areas) and alterations in the total mass of microtubule (MT) and F-actin polymer were measured. Our results show that cell adhesion to ECM induces changes in the assembly of MTs and MFs; however, large-scale alterations in cell form do not appear to be driven directly by these polymerization events. Rather, MFs and MTs appear to function as a single, structurally integrated unit which changes its form in response to changes in cell-ECM binding.

MATERIALS AND METHODS

Cell culture

Hepatocytes were isolated from adult male Wistar rats by collagenase perfusion and cultured as previously described (Mooney et al., 1992). Serum-free William's E medium (Gibco, Grand Island, NY) containing insulin (20 mU/ml; Sigma), epidermal growth factor (10 ng/ml; Collaborative Research, Bedford, MA), dexamethasone (5 nM; Sigma), sodium pyruvate (20 mM; Gibco), a mixture of penicillin and streptomycin (100 U/ml; Irvine Scientific, Santa Ana, CA), and ascorbic acid (50 μg/ml, fresh daily; Gibco) was used for all experiments. Hepatocytes were cultured on 60 mm bacteriological dishes (Becton Dickinson, Lincoln Park, NJ) for quantitation of tubulin levels, 24-well bacteriological dishes (Corning; Corning, NY) for quantitation of spreading kinetics, and glass Lab-Tek slides (Nunc; Naperville, IL) for immunofluorescence studies. The same ECM-density dependent control over cell spreading was found, regardless of the dish utilized. Dishes were pre-coated with defined and stable ECM densities varying from 1 to 1000 ng/cm^2 as previously described (Mooney et al., 1992). Laminin (LM; Collaborative Res., Bedford, MA), fibronectin (Cappel, Malvern, PA), type I collagen (Collagen Corp., Palo Alto, CA) and type IV collagen (Collaborative) were used. Cell plating densities were varied to obtain approximately 2500 adherent cells/cm^2 at all assay times (Mooney, 1992). In certain experiments, nocodazole (Aldrich Chemical Co.; Milwaukee, WI), cytochalasin D (Aldrich), or taxol (Calbiochem; La Jolla, CA) was added to the cell suspension, and the cells were incubated at 37°C for 30 minutes before plating. Cells were similarly preincubated and cultured in cycloheximide (Sigma) at a saturating concentration of 20 μg/ml to inhibit protein synthesis; this concentration inhibits protein synthesis by more than 85% in cultured hepatocytes (Mooney, 1992).

Morphological techniques

Adherent cells were fixed in glutaraldehyde (Electron Microscopy Sciences; Fort Washington, PA), dehydrated with methanol, and air dried. Photographic images of hepatocytes were recorded on Kodak Pan X 100 film using Hoffman optics on a Zeiss inverted microscope. Projected cell areas were measured in cells that were fixed and stained with Coomassie brilliant blue (Aldrich) using a computerized image analysis system, as previously described (Ingber, 1990). A minimum of 50 cells were recorded on each experimental condition.

To localize F-actin within MFs, adherent cells were fixed in 2% paraformaldehyde in PBS and stained with rhodamine-phalloidin (Molecular Probes, Eugene, OR) for 10 minutes. To analyze changes in MT distribution, cells were fixed in a MT stabilization buffer (MSB) (Caron et al., 1985), exposed to cold MeOH, and permeabilized with 0.2% Triton X-100 (Kodak) in PBS. MSB contained 0.1 M Pipes, pH 6.75, 1 mM EGTA, 1 mM $MgSO_4$, 2 M glycerol, and protease inhibitors (10 mg/ml leupeptin, 10 mg/ml aprotinin, 0.5 mM benzamidine, 5 mg/ml pepstatin A, 5 mg/ml *o*-phenanthroline, 0.5 mM phenylmethylsulfonyl fluoride). These chemicals were obtained from Sigma Chemical (Pipes, EGTA, benzamide, *o*-phenanthroline), BRL (glycerine), and Boehringer Mannheim (leupeptin, aprotinin, pepstatin, phenylmethysulfonyl fluoride). MTs were visualized by exposing cells to rabbit anti-bovine brain tubulin antibody (Biomedical Technologies Inc., Stoughton, MA) for 1 hour, washing 4 times with PBS, and exposing to rhodamine-conjugated goat anti-rabbit IgG (Organon Teknika, West Chester, PA). After staining, cells were covered with a polyvinyl alcohol/glycerol solution (Gelvatol; Monsanto Corp.), and overlaid with glass coverslips. Photographic images of cells stained for tubulin and F-actin were recorded on Kodak TMAX-400 film using a Zeis Axiophot immunofluorescence microscope.

Quantitation of tubulin

Tubulin was extracted from cells using a previously published technique (Caron et al., 1985). Briefly, cells were washed in MSB, and incubated with MSB + 0.1% Triton X-100 to remove the monomeric tubulin. Polymeric tubulin (MTs) was isolated by solubilizing the remaining cytoskeleton in lysis buffer (25 mM Tris-HCl, pH 7.4, 0.4 M NaCl, 0.5% SDS). All extraction steps were performed at 37°C with pre-warmed reagents. Tubulin in cellular extracts was quantitated using a previously described dot-blot assay (Mooney et al., 1992, 1994). Serial dilutions of cellular extracts and bovine brain tubulin standard (generously provided by Dr Stephen Farmer) were loaded onto nitrocellulose paper using a 96-well minifold apparatus. Blotted proteins were exposed to a rabbit anti-bovine brain tubulin antibody (Biomedical Technologies Inc.), and to ^{125}I-conjugated donkey anti-rabbit Fab^2 (Amersham; Arlington Heights, IL). Individual dots were then cut out, counted in a gamma counter, and the relative amount of tubulin was determined by comparison with values from the linear portion of a calibration curve calculated using the known amounts of the bovine brain tubulin standard. The mass of cellular tubulin was normalized for cell number by determining the number of cells attached in parallel plates using a Coulter counter. The specificity of the antibody against hepatocyte tubulin was confirmed by western blot analysis (not shown). Since this antibody may not have the same affinity for rat hepatocyte tubulin as for the bovine brain tubulin standard, the values for tubulin mass should be considered relative values.

Quantitation of F-actin mass

To allow precise quantitation of cellular F-actin content, and allow fast analysis of multiple samples, a previously published technique based on phalloidin binding was adapted (Howard and Oresajo, 1985). At given times post-plating cells were washed with PBS, fixed with a solution of 3.7% formaldehyde (Electron Microscopy Sciences) in PBS, and permeabilized by incubation with 0.2% Triton X-100 in PBS. A solution containing 3×10^{-7} M rhodamine-phalloidin (Molecular Probes, Eugene, OR) in the permeation buffer was then added to cells. After 10 minutes the wells were washed with PBS, and

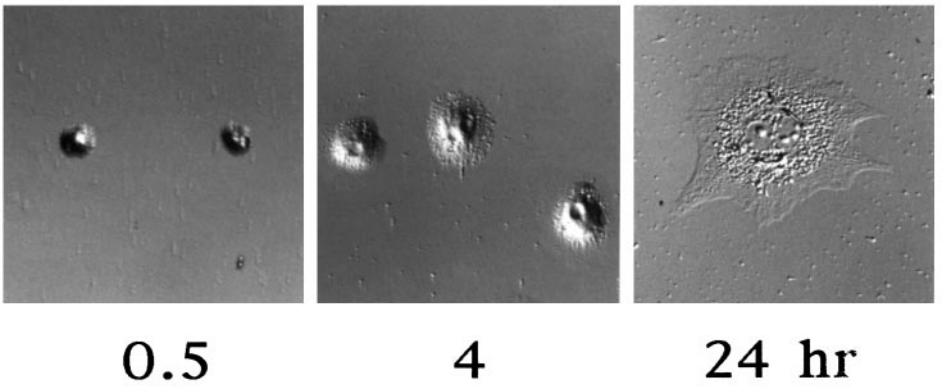

Fig. 1. Hepatocytes cultured in chemically defined medium on dishes coated with the high LM density (1000 ng/cm^2) for 0.5, 4 or 24 hours. All photomicrographs are printed at the same magnification (×160).

the bound rhodamine-phalloidin was subsequently solubilized by incubation with methanol (0.2 ml/well) for 1 hour in the dark. The methanol was removed from each well, placed in a 96-well plate, and the amount of extracted rhodamine-phalloidin was determined by measuring the rhodamine signal with a Fluorescence Concentration Analyzer (Baxter; Mendelin, IL). Examination of cells with an immunofluorescence scope after the methanol iμncubation confirmed the complete removal of phalloidin from cells. Cells in parallel wells were counted to normalize for cell number. To determine the initial quantity of F-actin in suspended cells prior to plating, a known number of cells was fixed, permeabilized, and suspended in the rhodamine-phalloidin solution. The cells were pelleted by centrifugation after 10 minutes, the rhodamine-phalloidin solution was removed, and the cells washed twice with PBS. The cells were resuspended in methanol and incubated for 1 hour at room temperature in the dark. The cells were again centrifuged, the methanol collected, and the extracted rhodamine signal in the methanol was read with the Fluorescence Concentration Analyzer. Western blot analysis of proteins extracted from cytoskeletal preparations of suspended and adherent cells confirmed the accuracy of this method for quantitating changes in cellular F-actin content (not shown).

Quantitation of albumin secretion

Hepatocytes were cultured in complete medium on 35 mm dishes coated with 1000 ng/cm^2 of LM. Nocodazole (10 μg/ml) was included in the medium during the first 6 hours of culture in one series of dishes; these cells were then washed free of drug and cultured in control medium for the remainder of the experiment. Secretion of albumin was quantitated using an ELISA assay. Medium samples were collected over a 24 hour period, and serially diluted into a 96-well dish pre-coated with a solution of 2 μg/ml of a rabbit anti-rat albumin polyclonal antibody (Cappel; Durham, NC) in a carbonate buffer (15 mM Na_2CO_3, 35 mM $NaHCO_3$, pH 9.6). Serial dilutions of rat albumin standard (Cappel) were also loaded in parallel on each plate. After 1 hour, non-bound proteins were removed with a PBS wash, and plates were exposed to a peroxidase-conjugated rabbit anti-rat albumin (Cappel). The unbound antibody was washed away after 1 hour, and the substrate for peroxidase (ABTS substrate (Sigma) in a buffer containing 61 mM citrate, 77 mM Na_2HPO_4, 0.01% H_2O_2) was added to the dish. The reaction was stopped after 45 minutes by adding sufficient sodium fluoride to yield 0.16%, and the extent of

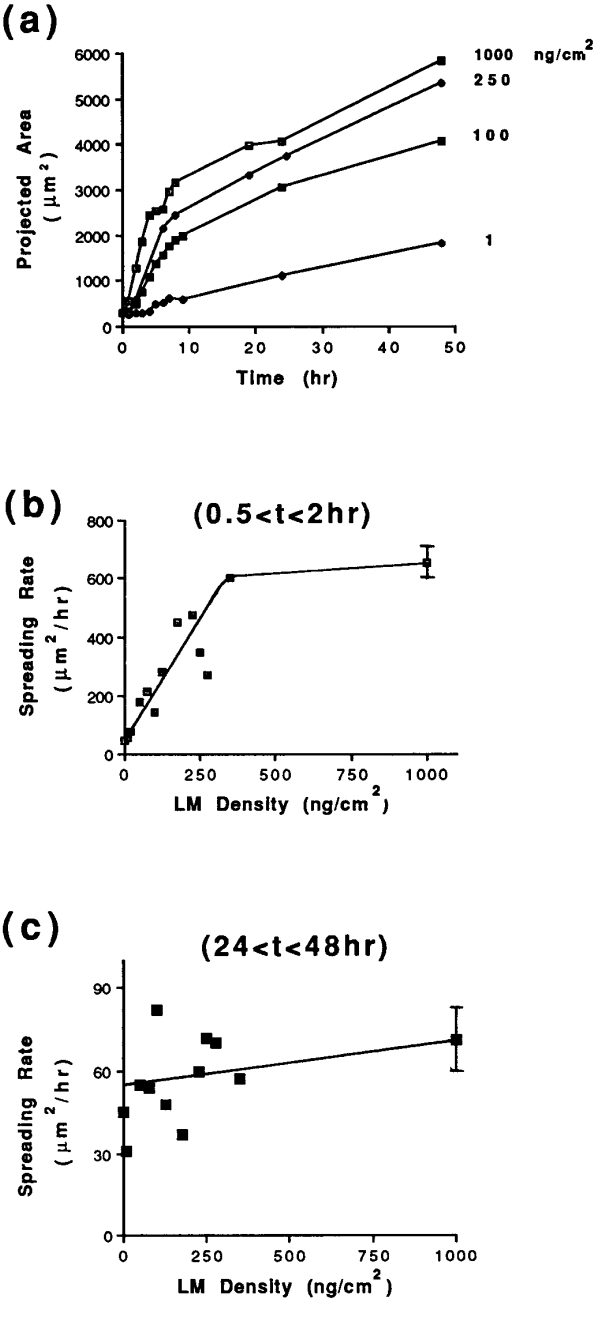

Fig. 2. (a) A representative experiment showing the kinetics of hepatocyte cell spreading on different LM densities. (b) The initial spreading rate measured at 0.5 to 2 hours after plating was highly dependent on the LM density used for cell attachment. (c) The cell spreading rate was independent of LM density at later times (24-48 hours). Data in (b) and (c) were from 4 separate measurements; all error bars indicate s.e.m.

reaction was determined by measuring the absorbance at 405 nm (versus 490 nm). Cells in parallel wells were again counted to normalize for cell number.

RESULTS

Control of hepatocyte spreading by ECM

Freshly isolated rat hepatocytes were cultured on dishes coated with various types and densities of ECM molecules to study the role of the ECM in regulating cell spreading. Hepatocytes plated on dishes coated with a high density of LM (1000 ng/cm^2) attached but remained round for the first half-hour following cell adhesion. The cells spread considerably by 4 hours and exhibited a highly extended and flattened morphology by 24 hours (Fig. 1). Subsequent experiments revealed that the rate and extent of hepatocyte spreading was controlled by the density of LM molecules on the culture surface (Fig. 2a). Cells on a low LM density (1 ng/cm^2) exhibited an average projected area of 1900 ± 600 μm^2 after 48 hours, while cells on a high LM density (1000 ng/cm^2) had an area of 6100 ± 840 μm^2. The magnitude of the initial spreading rate (0.5-2 hours) increased in a dose-dependent manner as the LM density was raised, with maximal rates being observed at densities above approximately 375 ng/cm^2 (Fig. 2b). A progressive transition to a slower rate of spreading (from 90 to 30 μm^2/h) was observed at approximately 4 to 6 hours (Fig. 2a) whereas, at later times, the spreading rate appeared to be independent of the LM density (Fig. 2c). Cells on the lowest LM densities (1-10 ng/cm^2) had a longer lag before cell extension began, but again exhibited a similar transition from a rapid to a slower spreading rate about 4-6 hours after spreading had initiated. Hepatocytes were cultured on various ECM molecules to determine whether this spreading profile was specifically due to adhesion to LM, or if it was a general response of hepatocytes adhering to ECM-coated surfaces. When hepatocytes were cultured on a saturating density of fibronectin, type I collagen or type IV collagen, a similar spreading profile was measured (Fig. 3) as well as a similar dependence on ECM density (not shown). Similar ECM-dependent control of cell spreading also was observed when cells were pretreated and cultured in the presence of cycloheximide to inhibit new protein deposition (not shown).

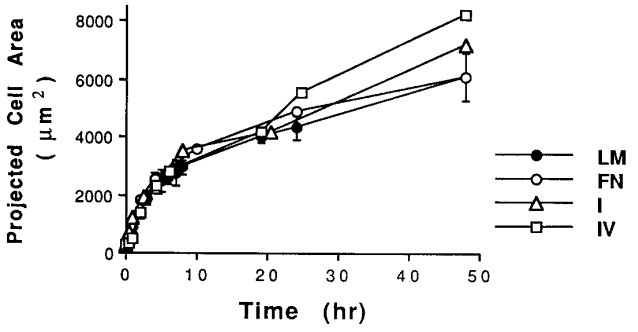

Fig. 3. The spreading kinetics of hepatocytes cultured on dishes coated with 1000 ng/cm^2 of LM, fibronectin (FN), type I collagen (I), or type IV collagen (IV). Error bars are only shown for cells on LM; the variations in projected areas for cells on the other ECM molecules were of a similar magnitude.

Adhesion-dependent changes in cytoskeletal filament assembly

To begin to address the question of whether cytoskeletal filament assembly drives hepatocyte spreading on ECM, we quantitated changes in the total mass and distribution of F-actin and MTs during the period following cell plating. Rhodamine-phalloidin labelling of F-actin in hepatocytes adherent to a high density of LM (1000 ng/cm^2) revealed bright, amorphous staining throughout the cell at 0.5 hour after cell plating (Fig. 4). This staining pattern was presumably due to a high density of F-actin fibers in the round cell. After 4 hours, the intensity of the staining was somewhat reduced, although the central portion of the cell remained brightly stained, with discrete actin filaments being visible at the cell periphery. At 24 hours, the highly extended cells exhibited a marginal actin band at its periphery with less intense amorphous and fine fibrillar staining throughout the remainder of the cell.

Changes in F-actin assembly were quantitated using a fluorescent phalloidin-binding assay. The total cellular F-actin mass was found to increase approximately 20-fold within 0.5 hour after hepatocytes attached to a high ECM density (1000 ng/cm^2) (Fig. 5a) even though the cells did not significantly change shape at this time (Figs 1 and 2a). Progressive disassembly of F-actin occurred over the subsequent 4-6 hours, within minimal changes in F-actin mass being observed after this time (Fig. 5a). A similar wave of assembly and disassembly was also found within cells cultured on lower densities of LM (Fig. 5b), although this effect was delayed slightly in cells on the lowest LM density, which also exhibited a delay in the onset of spreading (Fig. 2a). Neither the increase nor decrease in F-actin mass required new protein synthesis, as treatment of cells with cycloheximide had no effect on this rapid wave of

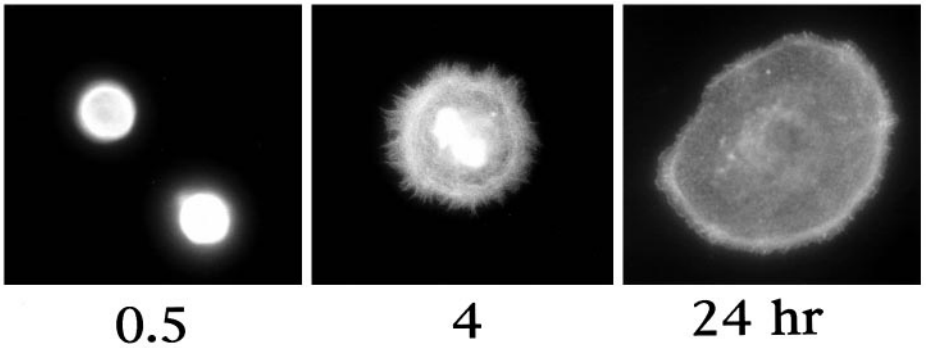

Fig. 4. Immunofluorescence microscopic view of rhodaminated-phalloidin staining for F-actin in hepatocytes cultured for 0.5, 4 and 24 hours on the high LM density. All photomicrographs were exposed for the same period of time and printed at the same magnification (×500).

polymerization and depolymerization (Fig. 5c). The F-actin mass remained relatively constant in cells on an intermediate ECM density over the ensuing 48 hours, decreased gradually in cells on the low ECM, and slowly increased on high (not shown).

Cell adhesion to ECM had different effects on MT assembly. Visualization of the MT array using indirect immunofluorescence microscopy and anti-tubulin antibodies revealed amorphous staining filling the cytoplasm of cells at 1 and 6 hours following adhesion, again presumably due to the presence of tightly packed MT filaments (Fig. 6). At 6 hours, a few individual MTs were also visible at the cell border, and by 24 hours a highly extended array of individual MTs appeared, extending radially from the perinuclear area to the cell periphery (Fig. 6). Quantitation of the MT mass in these cells using an immunoblotting assay revealed that the total mass of MT increased by 50% over the first 4 hours in culture (Fig. 7a), but decreased after this time to a value that remained constant for the duration of the experiment. Inhibition of protein synthesis using cycloheximide completely prevented the early rise in MT polymerization (Fig. 7b); however, it only partly inhibited hepatocyte spreading (Fig. 7c). Cycloheximide treatment also did not interfere with the transition from a rapid to a slower spreading rate at 4-6 hours.

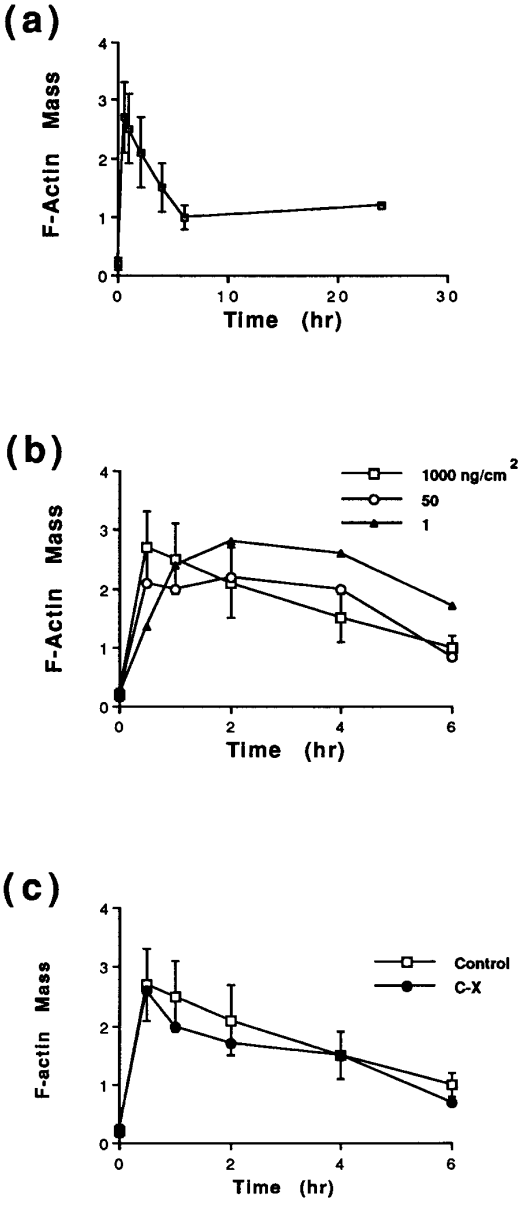

Fig. 5. (a) Time course of F-actin assembly in cells plated on dishes coated with high LM. (b) Effects of varying ECM density on the early phase of F-actin assembly and disassembly. A similar increase and subsequent decrease in F-actin mass was found when cells were cultured on high, moderate or low LM density (1000, 50 or 1 ng/cm^2, respectively). (c) Effects of cycloheximide (20 μg/ml; C-X) on F-actin mass in cells on cultured on high LM. Error bars for data points from control cells on 1000 ng of LM/cm^2 are shown; error bars for other conditions were of a similar magnitude. F-actin mass is expressed in arbitrary fluorescence units.

Cytoskeletal requirements for cell spreading

Although the rise in F-actin assembly did not correlate with cell extension, intact MFs were required for cell spreading. Addition of cytochalasin D, a drug which disrupts the integrity of the MF lattice (Fox and Phillips, 1981) resulted in dose-dependent inhibition of cell spreading. For example, a suboptimal dose of cytochalasin D (0.1 μg/ml) inhibited spreading at 48 hours by approximately 50% whereas at 10 μg/ml complete inhibition of cell extension was observed (Fig. 8). In contrast, induction of MT disassembly using nocodazole only partially inhibited hepatocyte extension, even when used at a saturating dose (10 μg/ml) (Fig. 9a). The rate and extent of hepatocyte extension also was only partially inhibited when

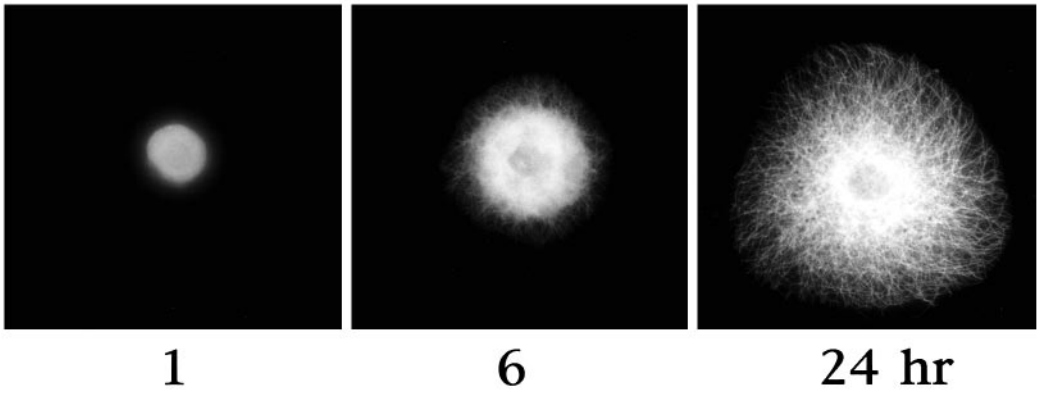

Fig. 6. Immunofluorescence microscopic view of tubulin staining in cells cultured on high LM for 1, 6 and 24 hours. All photographs were exposed for the same time and printed at the same magnification (×500).

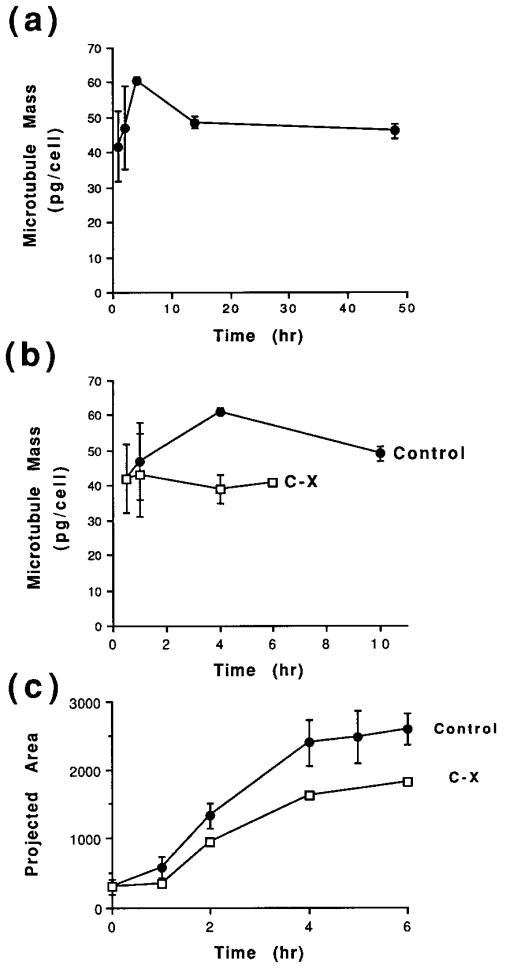

Fig. 7. Effects of ECM and cycloheximide on MT assembly and cell spreading. Changes in MT mass were quantitated using a dot-blot assay, as described in Materials and Methods. (a) Time course of MT assembly in cells on the high LM density. (b) Treatment of hepatocytes with cycloheximide (20 μg/ml) prevented the increase and subsequent decrease in MT mass following adhesion. (c) Treatment of cells with cycloheximide (C-X; 20 μg/ml) only slightly inhibited spreading at 6 hours.

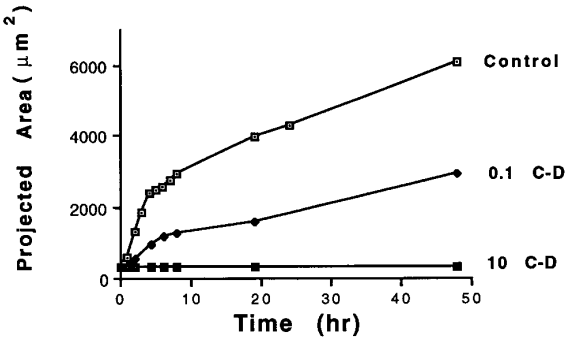

Fig. 8. Effect of cytochalasin D treatment on cell spreading on high LM. Hepatocyte spreading was partially inhibited by 0.1 μg/ml of cytochalasin D (0.1 C-D), and completely inhibited by 10 μg/ml (10 C-D).

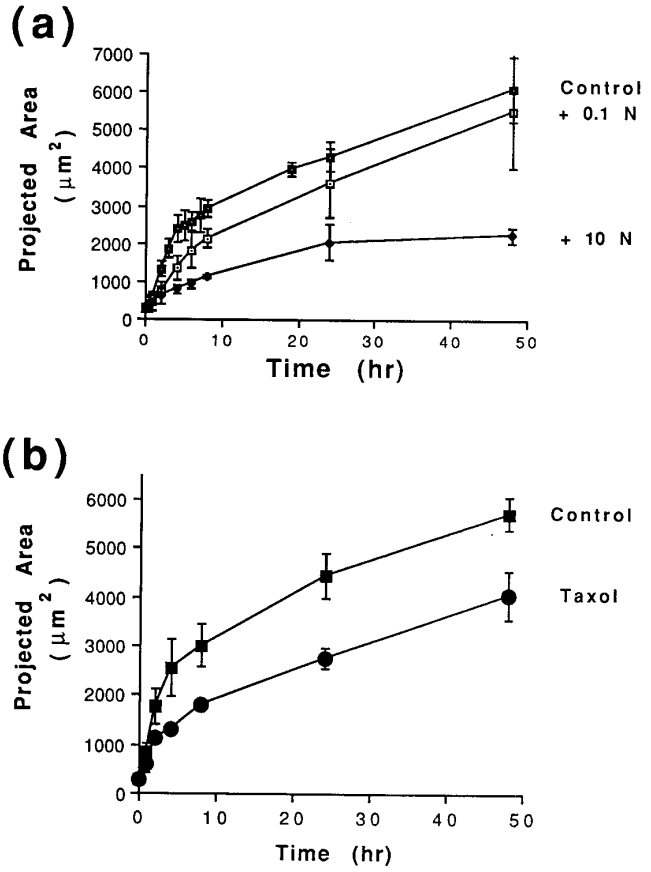

Fig. 9. Effects of MT-modifying drugs on cell spreading on high LM. (a) Hepatocyte spreading was partially suppressed when nocodazole was added at 0.1 μg/ml (0.1 N) and greatly inhibited at 10 μg/ml (10 N). (b) Exposure to taxol (15 μM) only resulted in a slight inhibition of hepatocyte spreading.

taxol was added (Fig. 9b). Taxol promotes MT polymerization but results in formation of a disorganized MT lattice. Immunofluorescence studies confirmed that treatment of hepatocytes with both drugs resulted in disruption of the normal MT lattice (Fig. 10). Nevertheless, the transition between rapid and slower spreading rate was still observed at approximately 4-6 hours after plating in both taxol- and nocodazole-treated cells (Fig. 9). Interestingly, nocodazole (10 μg/ml) completely prevented subsequent extension when it was added 8 or 24 hours after spreading had been initiated (Fig. 11a), even though the same dose only partially suppressed spreading when included during the initial attachment process (Fig. 9a). Immunfluorescence analysis revealed that most of the MTs at the cell periphery depolymerized when nocodazole was added at these later times; however, MT in the central portion of the cell appeared to remain intact (Fig. 11b).

These results with cytoskeleton-modifying drugs suggested that F-actin filaments provide a more significant supporting role during cell spreading than MTs. However, one possibility that has been raised is that there is significant structural redundancy in the cytoskeleton (Ingber, 1993; Ingber et al., 1994). Specifically, MTs may function as critical internal support struts during spreading; however, this function is taken over by intact actin filaments when MTs are compromised. To explore this possibility, cells were exposed to suboptimal doses of

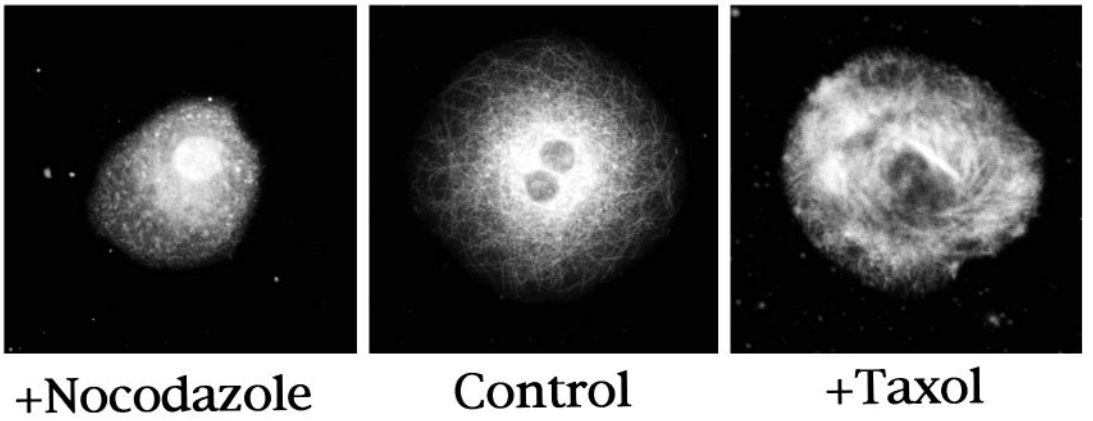

Fig. 10. Immunofluorescence microscopic view of tubulin staining in hepatocytes cultured for 48 hours on high LM and treated with nocodazole(10 μg/ml), control (no drug), or taxol (15 μM). All photomicrographs were printed at the same magnification (×500).

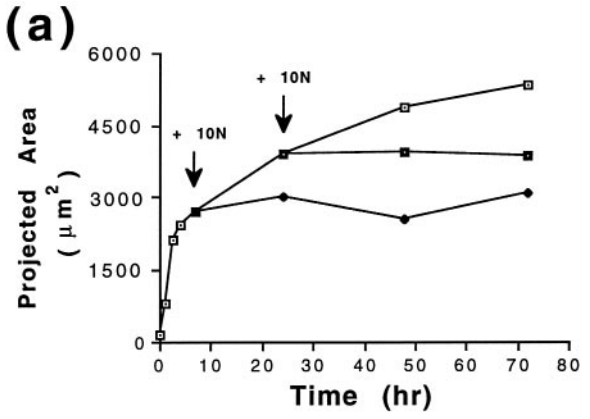

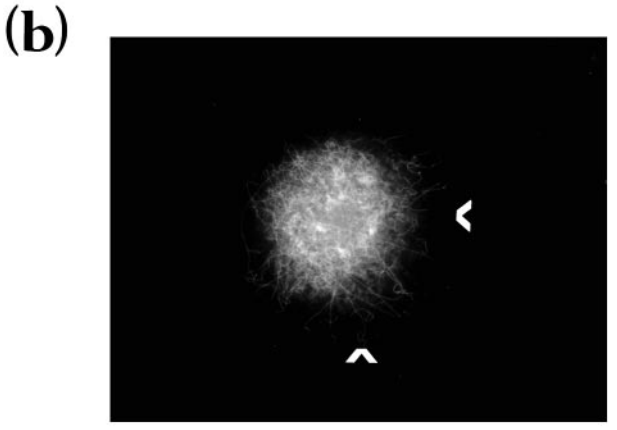

Fig. 11. (a) Effects of late addition of nocodazole on hepatocyte spreading kinetics and size on high LM. Exposure of hepatocytes to 10 μg/ml of nocodazole (10 N) beginning 8 or 24 hours after plating inhibited any further increase in projected cell area.
(b) Immunofluorescence microscopic view of tubulin in hepatocytes exposed to nocodazole (10 μg/ml) beginning 24 hours after plating on high LM. Tips of arrowheads abut on the periphery of a single, spread hepatocyte which retains distinct MT filaments only in its central region (×500).

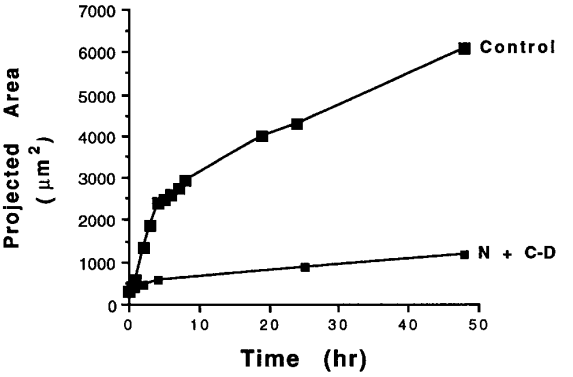

Fig. 12. Effects of combining suboptimal doses of cytochalasin D (0.1 μg/ml; C-D) and nocodazole (0.1 μg/ml; N) on hepatocyte spreading on high LM.

nocodazole (0.1 μg/ml) and cytochalasin D (0.1 μg/ml). When used alone at these doses, these drugs only partially inhibit cell extension. In contrast, when the drugs were added simultaneously, hepatocyte spreading was completely inhibited (Fig. 12).

The cytoskeleton and functional control

Studies were carried out to determine whether cytoskeleton-dependent changes in cell shape are critical for control of hepatocyte function. Hepatocytes were exposed to nocodazole for the first 6 hours of culture and were then refed with normal medium. This short-term treatment with nocodazole slowed the normally rapid early phase of spreading (Fig. 9a) and resulted in production of cells that were significantly smaller than controls 48 hours later, even though normal MT architecture was restored within hours after nocodazole was removed from the culture (not shown). The projected areas of treated and control cells at 48 hours was 4000 ± 500 μm^2 and 5700 ± 600 μm^2, respectively. The smaller, nocodazole-treated cells also exhibited a significantly higher rate of albumin secretion than untreated cells (115 ± 33 vs 54 ± 10 pg/cell per day at 48 hours) and this difference was maintained for 8 days in this experiment.

DISCUSSION

This study was undertaken to determine how cell binding to ECM-coated surfaces regulates cell spreading. Our results show that increasing the density of immobilized ECM ligand

results in a dose-dependent increase in the rate of cell spreading during the first few hours after plating. This initially rapid spreading rate slowed at approximately 4-6 hours and thereafter was independent of ECM density. Interestingly, this transition appeared to be triggered by adhesion per se, since it was observed on all ECM substrata regardless of type or coating density, in both the absence and presence of new protein synthesis. The early rapid phase of cell extension did not correlate with an increase in F-actin assembly, although disruption of the MF lattice using cytochalasin D completely prevented cell spreading. In contrast, a progressive increase in MT mass was observed over the first 4 hours of culture; however, inhibition of MT polymerization using nocodazole had only minor effects on cell extension. It also did not prevent the transition from ECM-dependent to independent spreading. Yet, the same dose of nocodazole completely inhibited cell extension when combined with a suboptimal dose of cytochalasin D. These results suggest that there is structural redundancy in the cytoskeleton in terms of its role in cell shape determination; that is, MFs can stabilize cytoskeletal form if MTs are partially compromised and vice versa. The importance of the cytoskeleton and cell shape for control of cell function was also confirmed by the finding that a brief exposure to nocodazole resulted in both decreased cell size and enhanced production of a liver-specific product many hours later.

Raising the ECM molecular coating density most likely increased the initial rate and extent of cell spreading by promoting formation of a higher number and density of adhesive bonds between immobilized ECM molecules and cell surface ECM receptors, such as integrins. The density of adhesive bonds is a function of the ECM coating concentration, the density of cell surface ECM receptors, and the binding affinity of these receptors. The ECM receptor density on hepatocytes has been estimated to be approximately 33 fmol/cm^2 using fibronectin as the ligand (Bissell et al., 1986), and equilibrium constants for this type of binding reaction range from 10^{12} to 10^{18} cm^2/mol (Hammer and Lauffenburger, 1989). Because there is saturation of cell receptors at high ECM coating densities there is a hyperbolic relation between the ECM coating concentration and the cell-ECM bond density for typical equilibrium constant values (Fig. 13). This prediction is consistent with the results of the present study in which the rate of cell spreading was saturated at high ECM densities (Fig. 2a). Nevertheless, it is unclear whether increasing the density of cell-ECM bonds accelerates cell spreading by promoting more rapid focal contact formation and cytoskeletal rearrangements (Massia and Hubbell, 1991), by more effectively resisting cell-generated tractional forces (Ingber, 1993), or by activating chemical signaling mechanisms (Schwartz, 1992).

The initially rapid spreading rate progressively slowed after plating and became independent of the ECM density after approximately 4-6 hours of culture, regardless of the type of ECM component used for cell attachment. There are several possible mechanisms by which cells could elicit these effects. For example, cells may become independent of the ECM coating density by depositing new ECM molecules and expressing different ECM receptors (Stamotoglou et al., 1987; Kato et al., 1992), by altering their mechanics and, hence, their ability to deform (Janmey et al., 1988; Wang et al., 1993), or by varying the forces that are generated in the cytoskeleton, which drive cell extension (Ingber, 1993; Ingber et al., 1994).

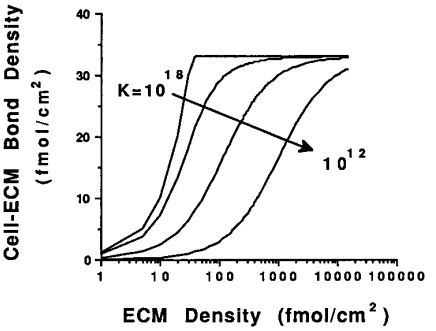

Fig. 13. Theoretical relationship between the ECM molecular coating density (ECM Density) and the density of adhesive bonds between cells and ECM (Cell-ECM Bond Density) for a range of values of the equilibrium constant for the binding reaction (K). The equilibrium bond density was calculated by writing a balance between bond formation and bond dissociation at steady state, and solving for bond density in terms of the ECM density, cell surface receptor density (assumed equal to 33 fmol/cm^2 for hepatocytes; Bissell et al., 1986), and typical equilibrium constants (K) for this type of reaction (10^{18} to 10^{12}; Hammer and Lauffenburger, 1989). For comparison with other figures, 1 ng LM/cm^2 equals 1.25 fmol LM/cm^2.

Inhibition of new protein synthesis only slightly decreased the spreading rate and had no effect on this time-dependent change in the spreading rate. Thus, expression of new receptors or production of a new ECM by the cells appear to be unlikely explanations for this finding.

Strikingly, variations in the mass of cellular MFs correlated temporally with changes in the spreading rate. However, the dramatic 20-fold increase in MF mass that was observed immediately following cell adhesion occured prior to the onset of cell spreading. This rapid increase in MF assembly following cell attachment to ECM may result from ECM-dependent increases in phosphatidylinositol bisphosphate (McNamee et al., 1993; Schwartz, 1992), which can compete with gelsolin and profilin for binding to G-actin (Janmey et al., 1987; Goldschmidt-Clermont et al., 1990) and thus, increase the local concentration of free actin monomer that is available for polymerization. Alternatively, actin polymerization could be induced as a result of recruitment and enrichment of molecules that can modify actin assembly (e.g. α-actinin, vinculin, talin) directly within the focal adhesion complex that forms at the site of ECM binding (Plopper and Ingber, 1993). The slower rate of MF assembly in cells on the lower ECM densities was also paralleled by a longer delay before spreading commenced. This delay may be related to the lower density of ECM-cell receptor bonds in cells cultured on these dishes or to a delay in focal adhesion formation. The cause of the subsequent decrease in MF mass is unclear, although oscillations in the MF content of activated neutrophils have been previously noted on a much shorter time scale (Wymann et al., 1990).

It is interesting that the most rapid phase of hepatocyte spreading was actually accompanied by a rapid wave of MF disassembly. Thus, outward extension of the cell periphery does not appear to be driven directly by a net increase in actin polymerization in these cells. However, the rate of cell spreading did progressively decrease during the phase of F-

actin disassembly. The total mass of MFs may dictate the magnitude of force that cells generate, due to the involvement of actomyosin interactions in the process of the force generation (Giuliano and Taylor, 1990; Kolega et al., 1991; Sims et al., 1993). At the same time, the MF system mechanically stabilizes cell extensions and is largely responsible for the stiffness of cultured cells (Wang et al., 1993; Ingber, 1993; Wang and Ingber, 1994). One possibility is that the initial large increase in F-actin mass may be necessary to generate enough force to overcome the mechanical resistance of the entire cytoskeleton so that cell deformation can proceed. This hypothesis is consistent with the finding that a similar increase in F-actin mass was induced, regardless of the ECM density, before cell deformation was observed (Fig. 5b). Although the mechanism for the subsequent decrease in F-actin mass is unknown, it would be expected to result in less total force generation and, hence, progressively slower rates of cell extension, as was observed. On the other hand, the rate of cell extension could be slowed due to increased cytoskeletal stiffness, caused by the mechanical stress-induced remodeling of the MF lattice that accompanies cell spreading (Wang et al., 1993; Ingber, 1993; Wang and Ingber, 1994). Of course, it is possible that both of these mechanisms come into play.

The observed change from rapid to slow spreading kinetics was also accompanied by a wave of MT assembly and disassembly. However, drug-induced disassembly of MTs did not alter this transition or prevent cell extension. These findings suggest that cells possess a compensatory mechanism for structurally stabilizing cell form when MTs are impaired. We have previously suggested that different cytoskeletal filament systems may provide redundant load-bearing functions and, specifically, that the MF lattice may be sufficient to stabilize cell structure when MTs are compromised (Ingber, 1993; Ingber et al., 1994). The observation that spreading was completely eliminated by simultaneous, partial impairment of MTs and MFs, but not by either perturbation alone, supports this argument. However, this compensatory mechanism apparently is less functional at later times or when cells are already highly extended on ECM, since addition of nocodazole many hours after plating resulted in complete inhibition of subsequent cell extension. MTs also have been found to provide more critical load-bearing functions in the most highly extended portions of the cell body in previous studies (Dennerll et al., 1988; reviewed by Ingber, 1993).

The possibility that MTs and ECM may play complementary load-bearing roles during cell spreading (Buxbaum and Heideman, 1988; Ingber and Folkman, 1989b; Lamoureux et al., 1990; Ingber, 1993) is also supported by this study. Depolymerization of MTs results in transfer of forces formerly supported by MT struts to the ECM via transmission across cell surface receptors (Danowski, 1989; Kolodney and Wysolmerski, 1992). The increased force on the cell receptor-ECM bonds would be expected to decrease the equilibrium constant for the binding (Hammer and Lauffenburger, 1989) and, thus, result in a decrease in the density of bonds that form. Thus, interference with MT assembly and decreasing the ECM molecular coating density of the substratum should have the same effect on cell spreading, as was observed in the present study (Figs 2a and 9a). Conversely, formation of increased numbers of cell receptor-ECM bonds could drive MT assembly during rapid cell spreading by reducing the compressive load that is born by MTs and, thereby, lowering the critical concentration for tubulin polymerization (Buxbaum and Heideman, 1988).

In past studies, it was shown that hepatocytes could be switched from differentiation to growth by culturing the cells on ECM substrata that differ in their ability to promote cell spreading (Mooney et al., 1992; Singhvi et al., 1994). In general, higher levels of differentiation-specific functions were exhibited by cells that were prevented from extending by modulating cell-ECM binding. Our results show that similar control of hepatocyte shape and function can be exerted by altering MT assembly (using nocodazole) and, hence, changing cytoskeletal organization. These results confirm that it is the degree of cell extension and not the method used to control spreading that determines the long-term function of cultured hepatocytes. However, it is important to note that the total steady state mass of MTs does not change when hepatocyte shape is altered (Mooney et al., 1994). Thus, the significance of cell 'shape' changes for cell function and control of gene expression may relate to associated changes in cytoskeletal organization and structure, rather than general alterations in cytoskeletal filament mass.

In summary, these data indicate that cell adhesion to ECM triggers the assembly and subsequently disassembly of MTs and MFs; however, cell spreading does not appear to be driven by net polymerization of either cytoskeletal filament system. Instead, these filament systems appear to act as a single, structurally integrated lattice which alters its form in response to changes in adhesive bond formation between cell surface receptors and immobilized ECM ligands.

The authors thank Dr Fontaine for her assistance in isolating hepatocytes, and Dr Hansen for helpful discussions. The tubulin protein standard was generously provided by Dr Stephen Farmer. This work was supported by grants from Advanced Tissue Sciences and NASA (NAG-9-430). Dr Ingber is a recipient of a Faculty Research Award from the American Cancer Society.

REFERENCES

Ben-Ze'ev, A. G., Robinson, S., Bucher, N. L. and Farmer, S. L. (1988). Cell-cell and and cell-matrix interactions differentially regulate the expression of hepatic and cytoskeletal genes in primary cultures of rat hepatocytes. *Proc. Nat. Acad. Sci. USA* **85**, 1-6.

Bereiter-Hahn, J., Luck, M., Miebach, T., Stelzer, H. K. and Voth, M. (1990). Spreading of trypsinized cells: cytoskeletal dynamics and energy requirements. *J. Cell Sci.* **96**, 171-188.

Bissell, D. M., Stamatoglou, S. C., Nermut, M. V. and Hughes, R. C. (1986). Interactions of rat hepatocytes with type IV collagen, fibronectin and laminin matrices. Distinct matrix-controlled modes of attachment and spreading. *Eur. J. Cell Biol.* **40**, 72-78.

Bissell, D. M., Arenson, D. M., Maher, J. J. and Roll, F. J. (1987). Support of cultured hepatocytes by a laminin rich gel. *Am. Soc. Clin. Invest.* **79**, 801-812.

Buxbaum, R. E. and Heidemann, S. R. (1988). A thermodynamic model for force integration and MT assembly during axonal elongation. *J. Theor. Biol.* **134**, 379-390.

Caron, J. M., Jones, A. L. and Kirschner, M. W. (1985). Autoregulation of tubulin synthesis in hepatocytes and fibroblasts. *J. Cell Biol.* **101**, 1763-1772.

Danowski, B. A. (1989). Fibroblast contractility and actin organization are stimulated by microtubule inhibitors. *J. Cell Sci.* **93**, 255-266.

Dennerll, T. J., Joshi, H. C., Steel, V. L., Buxbaum, R. E. and Heidemann, S. R. (1988). Tension and compression in the cytoskeleton of PC-12 neurites II: quantitative measurements. *J. Cell Biol.* **107**, 665-674.

Folkman, J. and Moscona, A. (1978). Role of cell shape in growth control. *Nature* **273**, 345-349.

Fox, J. E. B. and Phillips, D. R. (1981). Inhibition of actin polymerization in blood platelets by actin polymerization. *Nature* **292**, 650-652.

Giuliano, K. A. and Taylor, D. L. (1990). Formation, transport, contraction and disassembly of stress fibers in fibroblasts. *Cell Motil. Cytoskel.* **16**, 14-21.

Goldschmidt-Clermont, P. J., Machesky, L. M., Baldassare, J. J and Pollard, T. D. (1990). The actin-binding protein profilin binds to PIP_2 and inhibits its hydrolysis by phospholipase C. *Science* **247**, 1575-1578.

Hammer, D. A. and Lauffenburger, D. A. (1989). A dynamical model for receptor-mediated cell adhesion to surfaces in viscous shear flow. *Cell Biophys.* **14**, 139-173.

Howard, T. H. and Oresajo, E. O. (1985). A method for quantifying F-actin in chemotractic peptide activated neutrophils: study of the effect of tBOC peptide. *Cell Motil.* **5**, 545-557.

Ingber, D. E. and Folkman, J. (1989a). Mechanochemical switching between growth and differentiation during fibroblast growth factor-stimulated angiogenesis in vitro: role of extracellular matrix. *J. Cell Biol.* **109**, 317-330.

Ingber, D. E. and Folkman, J. (1989b). Tension and compression as basic determinants of cell form and function: utilization of a cellular tensegrity mechanism. In *Cell Shape, Determinants, Regulation and Regulatory Role* (ed. W. Stein and F. Bronner), pp. 1-32. San Diego: Academic Press.

Ingber, D. E. (1990). Fibronectin controls capillary endothelial cell growth by modulating cell shape. *Proc. Nat. Acad. Sci. USA* **87**, 3579-3583.

Ingber, D. E. (1993). Cellular tensegrity: defining new rules of biological design that govern the cytoskeleton. *J. Cell Sci.* **104**, 613-627.

Ingber, D. E., Dike, L., Hansen, L., Karp, S., Liley, H., Maniotis, A., McNamee, H., Mooney, D., Plopper, G., Sims, J. and Wang, N. (1994). Cellular tensegrity: exploring how mechanical changes in the cytoskeleton regulate cell growth, migration, and tissue pattern during morphogenesis. *Int. Rev. Cytol.* **150**, 173-224.

Janmey, P. A., Hvidt, S., Peetermans, J., Lamb, J., Ferry, J. D. and Stossel, T. P. (1988). Viscoelasticity of F-actin and F-actin/gelsolin complexes. *Biochemistry* **27**, 8218-8227.

Janmey, P. A., Iida, K., Yin, H. L. and Stossel, T. P. (1987). Polyphosphoinositide micelles and polyphosphoinositide-containing vesicles dissociate endogenous gelsolin-actin complexes and promote actin assembly from the fast-growing end of actin filaments blocked by gelsolin. *J. Biol. Chem.* **262**, 12228-12236.

Kato, S., Otsu, K., Ohtake, K., Kimura, Y. Yashiro, T., Suzuki, T. and Akamatsu, N. (1992). Concurrent changes in sinusoidal expression of laminin and affinity of hepatocytes to laminin during rat liver regeneration. *Exp. Cell Res.* **198**, 59-68.

Kolega, J., Janson, L. W. and Taylor, D. L. (1991). The role of solation-contraction coupling in regulating stress fiber dynamics in nonmuscle cells. *J. Cell Biol.* **114**, 993-1003.

Kolodney, M. and Wysolmerski, R. B. (1992). Isometric contraction by fibroblasts and endothelial cells in tissue culture: a quantitative study. *J. Cell Biol.* **117**, 73-82.

Lamoureux, P., Steel, V. L., Regal, C., Adgate, L., Buxbaum, R. E. and Heidemann, S. R. (1990). Extracellular matrix allows PC-12 neurite elongation in the absence of MTs. *J. Cell Biol.* **110**, 71-79.

Li, M. L., Aggeler, J., Farson, D. A., Hatier, C., Hassell, J. and Bissell, M. J. (1987). Influence of reconstituted basement membrane and its components on casein gene expression and secretion in mouse mammary epithelial cells. *Proc. Nat. Acad. Sci. USA* **84**, 136-140.

Massia, S. P. and Hubbell, J. A. (1991). An RGD spacing of 440 nm is sufficient for integrin $\alpha v\beta 3$-mediated fibroblast spreading and 140 nm for focal contact and stress fiber formation. *J. Cell Biol.* **114**, 1089-1100.

McNamee, H., Ingber, D. E. and Schwartz, M. A. (1993). Adhesion to fibronectin stimulates inositol lipid synthesis and enhances PDGF-induced inositol lipid breakdown. *J. Cell Biol.* **121**, 63-678.

Michalopoulos, G. and Pitot, H. C. (1975). Primary culture of parenchymal liver cells on collagen membranes. *Exp. Cell Res.* **94**, 70-78.

Mooney, D. J., Hansen, L. K., Farmer, S., Vacanti, J. P., Langer, R. and Ingber, D. E. (1992). Switching from differentiation to growth in hepatocytes: control by extracellular matrix. *J. Cell Physiol.* **151**, 497-505.

Mooney, D. J. (1992). Ph. D. thesis. Massachusetts Institute of Technology, p. 122-124.

Mooney, D. J., Hansen, L. K, Langer, R., Vacanti, J. P. and Ingber, D. E. (1994). Extracellular matrix controls tubulin monomer levels in hepatocytes by regulating protein turnover. *Mol. Biol. Cell* **5**, 1281-1288.

Opas, M. (1989). Expression of the differentiated phenotype by epithelial cells is regulated by both biochemistry and mechanics of substratum. *Dev. Biol.* **131**, 281-293.

Plopper, G. and Ingber, D. E. (1993). Rapid induction and isolation of focal adhesion complexes. *Biochem. Biophys. Res. Commun.* **193**, 571-578.

Schwartz, M. A. (1992). Transmembrane signalling by integrins. *Trends Cell Biol.* **2**, 304-308.

Sims, J., Karp, S. and Ingber, D. E. (1992). Altering the cellular mechanical force balance results in integrated changes in cell, cytoskeletal and nuclear shape. *J. Cell Sci.* **103**, 1215-1222.

Singhvi, R., Kumar, A., Lopez, G. P., Stephanopoulos, G. N., Wang., D. I. C., Whitesides, G. M. and Ingber, D. E. (1994). Engineering cell shape and function. *Science* **264**, 696-698.

Stamatoglou, S. C., Hughes, R. C. and Lindahl, U. (1987). Rat hepatocytes in serum-free primary culture elaborate an extensive ECM containing fibrin and fibronectin. *J. Cell Biol.* **105**, 2417-2425.

Stossel, T. P. (1989). From signal to pseupod: how cells control cytoplasmic actin assembly. *J. Biol. Chem.* **264**, 18261-18264.

Theriot, J. A. and Mitchison, T. J. (1991). Actin microfilament dynamics in locomoting cells. *Nature* **352**, 126-131.

Wang, N., Butler, J. P. and Ingber, D. E. (1993). Mechanotransduction across the cell surface and through the cytoskeleton. *Science* **260**, 1124-1126.

Wang, N. and Ingber, D. E. (1994). Control of cytoskeletal mechanics by extracellular matrix, cell shape, and mechanical tension. *Biophys. J.* **66**, 2181-2189.

Watt, F. M., Jordan, P. W. and O'Neill, C. H. (1988). Cell shape controls terminal differentiation of human epidermal keratinocytes. *Proc. Nat. Acad. Sci. USA* **85**, 5576-5588.

Wymann, M. P., Kernen, P., Bengtsson, T., Andersson, T., Baggiolini, M. and Deranleau, D. A. (1990). Corresponding oscillations in neutrophil shape and filamentous actin content. *J. Biol. Chem.* **265**, 619-622.

(Received 6 January 1995 - Accepted 22 March 1995)